Cha, Y., Jarrett-Wilkins, C., Rahman, M. A., Zhu, T., Sha, Y., Manners, I., & Tang, C. (2019). Crystallization-Driven Self-Assembly of Metallo-Polyelectrolyte Block Copolymers with a Polycaprolactone Core-Forming Segment. *ACS Macro Letters*, *8*, 835-840. https://doi.org/10.1021/acsmacrolett.9b00335

Crystallization-Driven Self-Assembly of Metallo-Polyelectrolyte Block Copolymers with a Polycaprolactone Core-Forming Segment

Yujin Cha,[†] Charlie Jarrett-Wilkins,[‡] Md Anisur Rahman,[†] Tianyu Zhu,[†] Ye Sha,[†] Ian Manners,[‡, ††,*] and Chuanbing Tang[†*]

[†]Department of Chemistry and Biochemistry, University of South Carolina, Columbia, South Carolina, 29208, United States

[‡]School of Chemistry, University of Bristol, Cantock's Close, Bristol BS8 1TS, United Kingdom

[††]Department of Chemistry, University of Victoria, 3800 Finnerty Road, Victoria BC, V8P 5C2, Canada

Supporting Information Placeholder

ABSTRACT: We report crystallization-driven self-assembly (CDSA) of metallo-polyelectrolyte block copolymers that contain cationic polycobaltocenium in the corona-forming block and crystallizable polycaprolactone (PCL) as the core-forming block. Dictated by electrostatic interactions originating from the cationic metalloblock and crystallization of the PCL, these amphiphilic block copolymers self-assembled into two dimensional platelet nanostructures in polar protic solvents. The 2D morphologies can be varied from elongated hexagons to diamonds, and their stability to fragmentation was found to be dependent on the ionic strength of the solution.

Self-assembly of amphiphilic block copolymers is one of the most fascinating approaches to the creation of nanoscale micelles with core-corona architectures and a broad range of morphologies.[1] Unlike amorphous block copolymers, when placed in a selective solvent, block copolymers with a crystallizable core-forming block tend to form micelles with a low curvature of the core-corona interface. Most commonly either platelets or cylinders are formed, depending on the interplay between the crystallization of the core and interchain repulsion of corona. The central role of crystallization in the self-assembly process has given rise to the descriptor "Crystallization-Driven Self-Assembly (CDSA)".[2]

Metallopolymers, polymers containing metal centers in the main chain or pendant side chains, have also been featured in CDSA processes. The CDSA of poly(ferrocenyldimethylsilane) (PFS) to prepare a wide range of nanostructures that are spherical, cylindrical[3] or platelet[4] micelles has been extensively explored. To date, most metallopolymers used for CDSA studies have been neutral. In contrast to neutral PFS, cationic cobaltocenium-containing polymers have several advantages, such as hydrophilicity, high chemical stability, and bioactivities.[4d, 5] As charged polyelectrolytes, cobaltocenium moieties have been utilized for solution self-assembly, including in one case for CDSA which gave platelets with a PFS core.[6] Recently, Qiu, Manners and coworkers reported the formation of chiral metallopolymers consisting of poly(cobaltoceniumethylene) with the assistance of *N*-acyl-amino-acid-derived anionic surfactants.[7] The Tang group have also reported the preparation and solution self-assembly of side-chain cobaltocenium-containing block copolymers in a mixture of acetone and chloroform that formed high-aspect-ratio nanotubular structures.[8]

Polycaprolactone (PCL) is well known for biomedical applications because of its biocompatibility and biodegradability.[9] PCL-containing block copolymers have been recently utilized for the CDSA process with the formation of spherical, cylindrical and lozenge-shaped morphologies.[10]

Scheme 1. Illustration of CDSA of PCL-*b*-PCoAEMA block copolymer toward hexagonal platelet

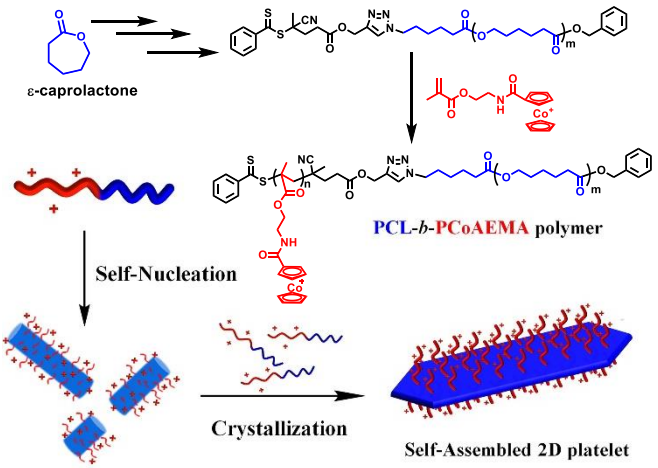

Herein we report the CDSA behavior of a metallo-polyelectrolyte block copolymer, polycaprolactone-*b*-poly(cobaltocenium amidoethyl methacrylate) (PCL-*b*-PCoAEMA). Driven by the crystallization of PCL and the electrostatic interactions within charged polycobaltocenium segments, this block copolymer can self-assemble into various two-dimensional platelet morphologies in selective solvents with PCL as the core block and cobaltocenium as the corona block (**Scheme 1**).

The cobaltocenium-containing block copolymer was synthesized via sequential ring-opening polymerization (ROP) of caprolactone and reversible addition-fragmentation chain transfer (RAFT) polymerization of cobaltocenium amidoethyl methacrylate hexafluorophosphate. PCL was synthesized via ROP and the terminal hydroxyl group was further converted to azide group, which was then subject to a click-type cycloaddition reaction with an acetylene-containing chain transfer agent (CTA), yielding dithioester-capped PCL as macro-CTA. CoAEMA monomer was then introduced as the second block via RAFT using the above macro-CTA. The compositions of block copolymers can be adjusted by changing the feed ratios of monomer to macro-CTA and were established by ^{1}H NMR. The solubility of cobaltocenium-containing block is largely dependent on its counterion.[11] In order to increase hydrophilicity of the corona-forming block, hexafluorophosphate counterion was exchanged to chloride by using tetrabutyl ammonium chloride, according to a previously reported procedure.[12]

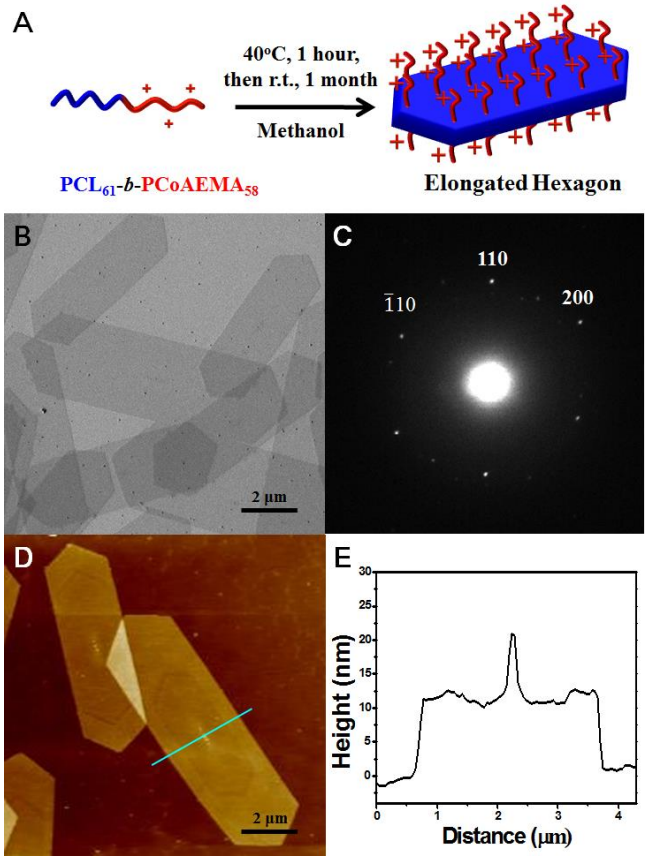

Figure 1. (A) Schematic illustration of the formation of 2D hexagonal platelets by CDSA of block copolymer PCL$_{61}$-*b*-PCoAEMA$_{58}$; (B) TEM micrograph of hexagonal platelets from PCL$_{61}$-*b*-PCoAEMA$_{58}$ obtained by heating the polymer solution in methanol at 40 °C for 1 hour followed by cooling and aging at room temperature for 1 month; (C) TEM SAED of hexagonal platetes; (D) AFM height image; (E) AFM height profile from image D.

First, we explored the self-assembly of the metallo-polyelectrolyte block copolymer with a short polycobaltocenium block (PCL$_{61}$-*b*-PCoAEMA$_{58}$). This block copolymer was dissolved in methanol with a concentration of 0.5 mg/mL, heated at 40 °C for 1 hour, and then slowly cooled to room temperature over 5 hours. Methanol was selected as the solvent because it is selective for the cobaltocenium block. The polymer solution was then aged at room temperature for one month and characterized by transmission electron microscopy (TEM) after solvent evaporation. TEM revealed the formation of platelets with a highly regular hexagonal shape and an average area of 19.6 μm^2 and a dispersity of A_w/A_n 1.24, where A_w is the weight-average area and A_n is the number-average area. (**Figures 1 and S9**). Selected area electron diffraction (SAED) from these hexagonal platelets showed that they possess a crystalline PCL core-forming block (**Figure 1C**). The diffraction pattern is in accordance with those previously reported.[13] Atomic force microscopy (AFM) clearly revealed that the hexagonal platelets have a thickness of ~10 nm. The linear zig-zag extended chain length of the PCL block is approximately 60 nm, which indicates the crystalline core contains chains that are folded ca. 6 times. Moreover, AFM analysis showed a distinct 1D region of elevation at the center (**Figure 1D**), which likely represents the location of a seed formed during the initial, self-nucleation stage of CDSA, which has been previously located in cases of seeded growth.[4c, 4d, 14]

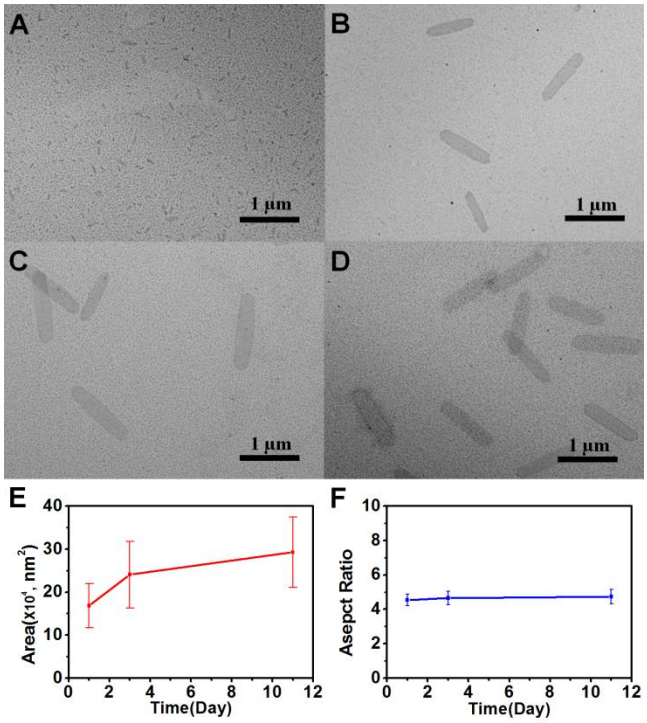

Figure 2. TEM micrographs of PCL$_{61}$-*b*-PCoAEMA$_{58}$ in methanol: (A) before heating; (B) aging for 1 day; (C) aging for 3 days; and (D) aging for 11 days. Plots of (E) area versus aging time and (F) aspect ratio versus aging time.

To further explore the CDSA behavior of this block copolymer during the aging, ^{1}H NMR experiments were carried out in methanol-d$_4$. Before starting the CDSA process (i.e. prior to heating), the proton peaks of solvated PCL to poly(cobaltocenium) showed a ratio of ca. 1:1 between two segments in the as-prepared block copolymer (**Figure S6**). As the aging proceeded, the intensity

of the proton peaks of PCL decreased whereas the proton peaks of cyclopentadienyl ring of cobaltocenium maintained unchanged (**Figure S16**). After aging for 11 days, the peak ratio of PCL to cobaltocenium reached ~0.4:1. As previously reported,[15] the protons at the α position of PCL are restricted and show a decreased intensity when the crystallization proceeds. The time-dependent CDSA process was also monitored by TEM. As shown in **Figure 2A**, when PCL_{61}-*b*-$PCoAEMA_{58}$ was dissolved in methanol without heating, TEM image shows small crystallites, which could serve as seeds for subsequent CDSA. Afterwards, the solution was subject to heating and aging as described above. After aging for 1 day, small elongated hexagonal platelets were formed (**Figure 2B**). With the increase of aging time, these hexagonal platelets grew larger (**Figure 2C-E**). The average area of hexagonal platelets after one-day aging was 1.68×10^5 nm^2. It increased to 2.41×10^5 nm^2 after 3 days and 2.92×10^5 nm^2 after 11 days. The area dispersity was 1.09. The aspect ratios (L_n/W_n, where L_n is the number-average length and W_n the number-average width) were similar, ca. 4.6, throughout the CDSA process.

Recent advances in self-assembly open a door for applications of micellar nanostructures in biomedical sciences. Chen and his coworkers showed that leaf-like 2D structures from poly(ethylene oxide)-*b*-polycaprolactone showed a selective permeability to different cells.[16] DeSimone and his coworkers demonstrated that nanoparticles with higher aspect ratios showed faster cellular internalizetion.[17] However, few stable 1D micellar systems in water by the CDSA process have been reported. Manners and coworkers reported cylindrical micelles that can be dialyzed from DMF to water.[18] Living CDSA of PCL-containing triblock in aqueous media reported by O'Reilly, Dove and coworkers.[10g] In terms of polyelectrolytes, cationic characteristics of the cobaltocenium block can play an important role on the colloidal stability of 2D structures in aqueous system. The salt responsiveness of quaternary ammonium-containing random copolymers has been previously described.[19] The increased ionic strength in aqueous solution can reduce the repulsive Coulomb interaction between cationic species.

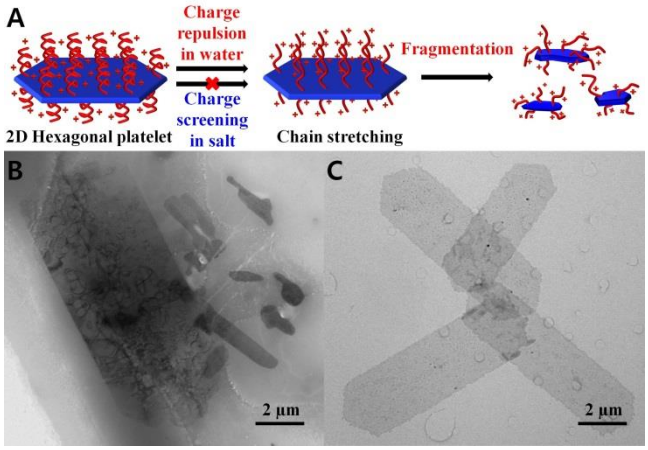

Figure 3. (A) Illustration of platelet fragmentation of PCL_{61}-*b*-$PCoAEMA_{58}$ caused by charge repulsion and preservation by charge screening in accordance with ionic strength; TEM micrographs: (B) fragmented hexagon by in methanol and water (v/v, 50/50), and (C) preserved hexagons by in methanol and 2.0 M NaCl aq. solution (v/v, 50/50).

In order to investigate the influence of electrostatic effects on the CDSA process, we changed the selective solvent from methanol to water, which would be expected to significantly enhance electrostatic repulsion between the cobaltocenium groups by increasing the solubility of the counterion. Following the same aging procedure, TEM analysis showed mainly the formation of small spherical micelles with a size of ~38 nm, consistent with 36.7 nm measured by Dynamic Light Scattering (**Figures S7 and S8**). This result suggests that the strong electrostatic repulsion of cationic cobaltocenium coronal segments in water induces maximum curvature of the core-corona interface to form spherical micelles where, as a result of the poorer quality of the solvent for PCL, rapid precipitation presumably leads to an amorphous core.

To provide further insight, we examined the effect of ionic strength on the formation of 2D platelets. Water was added to the solution of hexagonal platelets in methanol to give a volume ratio of methanol/water of 1/1. The hexagonal platelets were not stable and fragmented into smaller particles after 2 days (**Figure 3B**). However, when aqueous NaCl solution instead of pure water was added to the platelet micelle solution in methanol (volume ratio = 1/1, the final concentration of sodium chloride was 1.0 M), the hexagonal platelets, which have an area dispersity of 1.08, were preserved (**Figure 3C**). A series of solutions with different ionic strength were examined. The results indicated that an increase in ionic strength can screen repulsive interactions between the cationic cobaltocenium coronal chains and thus stabilize the platelets with respect to fragmentation.

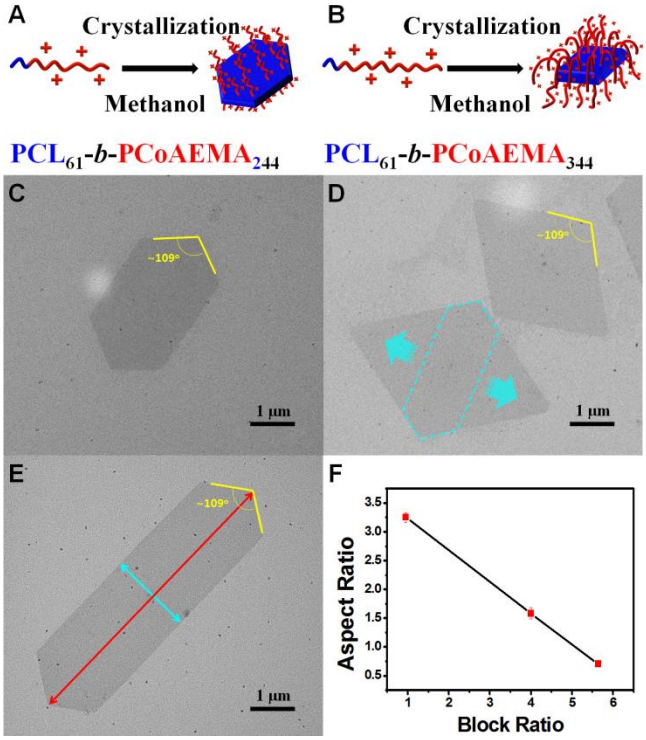

Figure 4. Schematic of (A, B) lower aspect ratio hexagonal platelet from PCL_{61}-*b*-$PCoAEMA_{244}$ and diamond-shaped platelet from PCL_{61}-*b*-$PCoAEMA_{344}$. TEM micrographs of platelets formed by (C) PCL_{61}-*b*-$PCoAEMA_{244}$ with an area dispersity of 1.05, (D) PCL_{61}-*b*-$PCoAEMA_{344}$ with an area dispersity of 1.11, and (E) PCL_{61}-*b*-$PCoAEMA_{58}$ in methanol and (F) plot of aspect ratio versus block ratio.

Next, we studied how the composition of block copolymers affected the CDSA process. We synthesized two block copolymers with a longer cobaltocenium block while keeping the degree of polymerization of the PCL block the same: PCL_{61}-*b*-$PCoAEMA_{244}$ and PCL_{61}-*b*-$PCoAEMA_{344}$. For amphiphilic block copolymers, an increased length of corona block can cause higher repulsion between chains, leading to larger interfacial curvature and thus resulting in morphological transformations.[3c, 20] We anticipated that the longer corona of the cobaltocenium block would induce the

morphological transition from 2D hexagonal platelets to 1D cylindrical or spherical morphologies. Self-assembly experiments were carried out using the same procedure as for PCL_{61}-*b*-$PCoAEMA_{58}$. However, TEM images showed that PCL_{61}-*b*-$PCoAEMA_{244}$ copolymer also produced hexagonal platelets which have an area dispersity of 1.05 with a larger width than that of PCL_{61}-*b*-$PCoAEMA_{58}$ (**Figures 4B and S12**). PCL_{61}-*b*-$PCoAEMA_{344}$ showed the formation of diamond-shaped platelets with an area dispersity of 1.11 (**Figures 4C and S13**) and lenticular shapes (**Figure S14**). Electron diffraction patterns of the wider hexagonal and diamond-shaped platelets revealed similar diffraction patterns to that of longer platelets (**Figures S12B and S13B**). We measured the angle of each platelet (depicted in yellow line in **Figure 4C-4E**). These 2D micelles share some common characteristics. As shown in **Figure 4**, the angle at the end of the elongated hexagon is ca. 110°, the wider hexagons and the diamond platelets exhibit the same angles at ~110°. The corners of 2D platelets were superimposed each other. To further characterize these 2D platelets, we measured aspect ratios of each platelet. Elongated hexagons from PCL_{61}-*b*-$PCoAEMA_{58}$, wider hexagons from PCL_{61}-*b*-$PCoAEMA_{244}$ and diamond-shaped platelets from PCL_{61}-*b*-$PCoAEMA_{244}$ have the aspect ratios respectively at 3.3, 1.6 and 0.7. The relationship between aspect ratio and block ratio showed a linear relationship (**Figure 4F**). As the block ratio increased, the aspect ratio decreased. AFM images of wider hexagonal and diamond-shaped platelets show the reduced thickness, 6 nm and 4 nm respectively (Figures S11D and S12D), suggesting increased chain folding compared to the narrow hexagonal case with a thickness of ca. 10 nm in Figure 1D and 1E. We postulated that when the corona block is short, the growth of platelets is dominated by the preferred unidirectional crystallization of the PCL block. It is likely that with the increase in the spatial extent of the corona, the rate of longitudinal crystallization is reduced by the presence of the hairy cobaltocenium segment, forcing platelets to expand more uniformly in both longitudinal and lateral directions. The increase in chain folding detected would also help stabilize the resulting platelets by reducing inter-coronal steric interactions by lowering the areal brush density. It appears that for this system this approach is favored over a reduction in the curvature of the core-corona interface to yield 1D fiber-like assemblies.

One of us reported diamond-shaped platelets from poly(L-lactide) homopolymers with a charged terminal phosphonium group.[4d] O'Reilly, Dove and coworkers described well-defined diamond platelets from poly(*N*,*N*-dimethylacrylamide)-*b*-P(L-lactide).[21] However, diamond platelets from a PCL-containing block copolymer have not yet been reported. It could be reasoned that the growth of 2D platelets is perpendicular to the axis of the long hexagonal platelet, as shown in **Figure 4D** (The dashed cartoon of hexagon). Although the reason of this phenomenon is not clear, we hypothesized that the direction of growth is governed by crystallization of the core-forming block. A 2D lamellar structure is accomplished by folding of the crystalline core block. The presence of a long corona block in a selective solvent can force more folding of PCL chains, as evidenced by the decrease of thickness of platelets via AFM imaging.

In order to further explore this phenomenon, we conducted additional experiments. It was reported that blending of crystalline homopolymers with block copolymers can accelerate the crystallization.[10b] We prepared a homopolymer of PCL_{38} and dissolved it in tetrahydrofuran at a concentration of 10 mg/mL. This solution was added to the diblock copolymer solution in methanol based on a mass ratio of 1:1. The blended solution was heated at 40 °C and cooled to room temperature slowly over 5 hours. TEM characterization was carried out after aging for 1 week. TEM images revealed that the addition of homopolymer resulted in longer hexagonal platelets (**Figure S15**). Blending with PCL_{61}-*b*-$PCoAEA_{58}$ in methanol resulted in elongated hexagonal platelets with a higher aspect ratio at ~7.8. For the diblock copolymers that formed wider hexagonal and diamond-shape platelets, they also showed long hexagonal platelets with higher aspect ratios at 6.67 and 6.52 respectively. Based on this observation, one might conclude that the increased crystallization rate of core-forming block induces the growth of 2D platelets along the longitudinal direction. The length of corona-forming block plays an important role in the shape formation of 2D platelets and the direction of growth.

In summary, cobaltocenium-containing metallo-polyelectrolyte block copolymers show some of unique crystallization-driven self-assembly behaviors in protic solvents that are selective for the polyelectrolyte block. The CDSA process resulted in exclusive 2D platelet structures including narrow and wide hexagons and diamonds. Moreover, the interplay between electrostatics of corona and crystallization of core dictates the transformation of morphologies, especially when coupled with block copolymer compositions. The platelets exhibited ionic strength-dependent stability in aqueous solutions. Recent efforts have revealed that 2D sharp nanostructures can penetrate, cross, or mechanically wrap microbial cells.[5g, 22] This feature, combined with the promising, previously reported biological behavior of cobaltocenium polymers, suggests that the 2D platelets described may open up new pathways toward biomedical applications.

ASSOCIATED CONTENT

Supporting Information

The Supporting Information is available free of charge on the ACS Publications website at http://pubs.acs.org.

Materials, experimental methods, characterization methods, synthesis schemes, NMR spectra, IR spectra, DLS profiles, TEM images and other additional information.

AUTHOR INFORMATION

Corresponding Author

*tang4@mailbox.sc.edu; ian.manners@bristol.ac.uk

Notes

The authors declare no competing financial interest.

ACKNOWLEDGMENT

This work is partially supported by the National Institutes of Health (Grant R01AI120987 to CT). The author would like to acknowledge the University of South Carolina Electron Microscopy Center for instrument use and technical assistance. IM thanks the Canadian Government for a Canada 150 Research Chair.

REFERENCES

1. (a) Cui, H.; Chen, Z.; Zhong, S.; Wooley, K. L.; Pochan, D. J., Block copolymer assembly via kinetic control. *Science* **2007,** *317* (5838), 647-50; (b) Discher, D. E.; Eisenberg, A., Polymer Vesicles. *Science* **2002,** *297* (5583), 967-973; (c) Li, Z.; Kesselman, E.; Talmon, Y.; Hillmyer, M. A.; Lodge, T. P., Multicompartment Micelles from ABC Miktoarm Stars in Water. *Science* **2004,** *306* (5693), 98-101; (d) Nie, Z.; Fava, D.; Kumacheva, E.; Zou, S.; Walker, G. C.; Rubinstein, M., Self-assembly of metal–polymer analogues of amphiphilic triblock copolymers. *Nat. Mater.* **2007,** *6*, 609; (e) Gröschel, A. H.; Walther, A.; Löbling, T. I.; Schacher, F. H.; Schmalz, H.; Müller, A. H. E., Guided hierarchical co-assembly of soft patchy nanoparticles. *Nature* **2013,** *503*, 247-251; (f) Warren, N. J.;

Armes, S. P., Polymerization-Induced Self-Assembly of Block Copolymer Nano-objects via RAFT Aqueous Dispersion Polymerization. *J. Am. Chem. Soc.* **2014,** *136* (29), 10174-10185; (g) Rodríguez-Hernández, J.; Chécot, F.; Gnanou, Y.; Lecommandoux, S., Toward 'smart' nano-objects by self-assembly of block copolymers in solution. *Prog. Polym. Sci.* **2005,** *30* (7), 691-724; (h) O'Reilly, R. K.; Hawker, C. J.; Wooley, K. L., Cross-linked block copolymer micelles: functional nanostructures of great potential and versatility. *Chem. Soc. Rev.* **2006,** *35* (11), 1068-1083; (i) Pochan, D. J.; Chen, Z.; Cui, H.; Hales, K.; Qi, K.; Wooley, K. L., Toroidal Triblock Copolymer Assemblies. *Science* **2004,** *306* (5693), 94-97.

2. (a) Qiu, H.; Hudson, Z. M.; Winnik, M. A.; Manners, I., Micelle assembly. Multidimensional hierarchical self-assembly of amphiphilic cylindrical block comicelles. *Science* **2015,** *347* (6228), 1329-32; (b) Schöbel, J.; Karg, M.; Rosenbach, D.; Krauss, G.; Greiner, A.; Schmalz, H., Patchy Wormlike Micelles with Tailored Functionality by Crystallization-Driven Self-Assembly: A Versatile Platform for Mesostructured Hybrid Materials. *Macromolecules* **2016,** *49* (7), 2761-2771; (c) Wang, J.; Zhu, W.; Peng, B.; Chen, Y., A facile way to prepare crystalline platelets of block copolymers by crystallization-driven self-assembly. *Polymer* **2013,** *54* (25), 6760-6767; (d) Pitto-Barry, A.; Kirby, N.; Dove, A. P.; O'Reilly, R. K., Expanding the scope of the crystallization-driven self-assembly of polylactide-containing polymers. *Polym. Chem.* **2014,** *5* (4), 1427-1436; (e) Choi, I.; Yang, S.; Choi, T.-L., Preparing Semiconducting Nanoribbons with Tunable Length and Width via Crystallization-Driven Self-Assembly of a Simple Conjugated Homopolymer. *J. Am. Chem. Soc.* **2018,** *140* (49), 17218-17225.

3. (a) Wang, X.; Guerin, G.; Wang, H.; Wang, Y.; Manners, I.; Winnik, M. A., Cylindrical block copolymer micelles and co-micelles of controlled length and architecture. *Science* **2007,** *317* (5838), 644-7; (b) Oliver, A. M.; Gwyther, J.; Winnik, M. A.; Manners, I., Cylindrical Micelles with "Patchy" Coronas from the Crystallization-Driven Self-Assembly of ABC Triblock Terpolymers with a Crystallizable Central Polyferrocenyldimethylsilane Segment. *Macromolecules* **2017,** *51* (1), 222-231; (c) Massey, J. A.; Temple, K.; Cao, L.; Rharbi, Y.; Raez, J.; Winnik, M. A.; Manners, I., Self-Assembly of Organometallic Block Copolymers: The Role of Crystallinity of the Core-Forming Polyferrocene Block in the Micellar Morphologies Formed by Poly(ferrocenylsilane-b-dimethylsiloxane) inn-Alkane Solvents. *J. Am. Chem. Soc.* **2000,** *122* (47), 11577-11584; (d) Gilroy, J. B.; Gadt, T.; Whittell, G. R.; Chabanne, L.; Mitchels, J. M.; Richardson, R. M.; Winnik, M. A.; Manners, I., Monodisperse cylindrical micelles by crystallization-driven living self-assembly. *Nat. Chem.* **2010,** *2* (7), 566-70.

4. (a) Qiu, H.; Gao, Y.; Boott, C. E.; Gould, O. E.; Harniman, R. L.; Miles, M. J.; Webb, S. E.; Winnik, M. A.; Manners, I., Uniform patchy and hollow rectangular platelet micelles from crystallizable polymer blends. *Science* **2016,** *352* (6286), 697-701; (b) Soto, A. P.; Gilroy, J. B.; Winnik, M. A.; Manners, I., Pointed-oval-shaped micelles from crystalline-coil block copolymers by crystallization-driven living self-assembly. *Angew. Chem. Int. Ed.* **2010,** *49* (44), 8220-3; (c) Nazemi, A.; He, X.; MacFarlane, L. R.; Harniman, R. L.; Hsiao, M. S.; Winnik, M. A.; Faul, C. F.; Manners, I., Uniform "Patchy" Platelets by Seeded Heteroepitaxial Growth of Crystallizable Polymer Blends in Two Dimensions. *J. Am. Chem. Soc.* **2017,** *139* (12), 4409-4417; (d) Yang, P.; Bam, M.; Pageni, P.; Zhu, T.; Chen, Y. P.; Nagarkatti, M.; Decho, A. W.; Tang, C., Trio Act of Boronolectin with Antibiotic-Metal Complexed Macromolecules toward Broad-Spectrum Antimicrobial Efficacy. *ACS Infect. Dis.* **2017,** *3* (11), 845-853; (e) Sha, Y.; Zhang, Y.; Zhu, T.; Tan, S.; Cha, Y.; Craig, S. L.; Tang, C., Ring-Closing Metathesis and Ring-Opening Metathesis Polymerization toward Main-Chain Ferrocene-Containing Polymers. *Macromolecules* **2018,** *51* (22), 9131-9139.

5. (a) Zhu, T.; Xu, S.; Rahman, A.; Dogdibegovic, E.; Yang, P.; Pageni, P.; Kabir, M. P.; Zhou, X. D.; Tang, C., Cationic Metallo-Polyelectrolytes for Robust Alkaline Anion-Exchange Membranes. *Angew. Chem. Int. Ed.* **2018,** *57* (9), 2388-2392; (b) Zhang, J.; Chen, Y. P.; Miller, K. P.; Ganewatta, M. S.; Bam, M.; Yan, Y.; Nagarkatti, M.; Decho, A. W.; Tang, C., Antimicrobial metallopolymers and their bioconjugates with conventional antibiotics against multidrug-resistant bacteria. *J. Am. Chem. Soc.* **2014,** *136* (13), 4873-6; (c) Ren, L.; Zhang, J.; Bai, X.; Hardy, C. G.; Shimizu, K. D.; Tang, C., Preparation of cationic cobaltoceniumpolymers and block copolymers by "living" ring-opening metathesis polymerization. *Chem. Sci.* **2012,** *3* (2), 580-583; (d) Qiu, H.; Gilroy, J. B.; Manners, I., DNA-induced chirality in water-soluble poly(cobaltoceniumethylene). *Chem. Commun.* **2013,** *49* (1), 42-4; (e) Pageni, P.; Yang, P.; Bam, M.; Zhu, T.; Chen, Y. P.; Decho, A. W.; Nagarkatti, M.; Tang, C., Recyclable magnetic nanoparticles grafted with antimicrobial metallopolymer-antibiotic bioconjugates. *Biomaterials* **2018,** *178*, 363-372; (f) Mayer, U. F.; Gilroy, J. B.; O'Hare, D.; Manners, I., Ring-opening polymerization of 19-electron [2]cobaltocenophanes: a route to high-molecular-weight, water-soluble polycobaltocenium polyelectrolytes. *J. Am. Chem. Soc.* **2009,** *131* (30), 10382-3; (g) Yan, Y.; Zhang, J.; Ren, L.; Tang, C., Metal-containing and related polymers for biomedical applications. *Chem. Soc. Rev.* **2016,** *45* (19), 5232-5263; (h) Zhu, T.; Sha, Y.; Yan, J.; Pageni, P.; Rahman, M. A.; Yan, Y.; Tang, C., Metallo-polyelectrolytes as a class of ionic macromolecules for functional materials. *Nat. Comm.* **2018,** *9* (1), 4329.

6. (a) Ren, L.; Zhang, J.; Hardy, C. G.; Ma, S.; Tang, C., Cobaltocenium-containing block copolymers: ring-opening metathesis polymerization, self-assembly and precursors for template synthesis of inorganic nanoparticles. *Macromol Rapid Commun* **2012,** *33* (6-7), 510-6; (b) Gilroy, J. B.; Patra, S. K.; Mitchels, J. M.; Winnik, M. A.; Manners, I., Main-Chain Heterobimetallic Block Copolymers: Synthesis and Self-Assembly of Polyferrocenylsilane-b-Poly(cobaltoceniumethylene). *Angew. Chem. Int. Ed.* **2011,** *50* (26), 5851-5855.

7. Musgrave, R. A.; Choi, P.; Harniman, R. L.; Richardson, R. M.; Shen, C.; Whittell, G. R.; Crassous, J.; Qiu, H.; Manners, I., Chiral Transmission to Cationic Polycobaltocenes over Multiple Length Scales Using Anionic Surfactants. *J. Am. Chem. Soc.* **2018,** *140* (23), 7222-7231.

8. Ren, L.; Hardy, C. G.; Tang, C., Synthesis and solution self-assembly of side-chain cobaltocenium-containing block copolymers. *J Am Chem Soc* **2010,** *132* (26), 8874-5.

9. Tian, H. Y.; Tang, Z. H.; Zhuang, X. L.; Chen, X. S.; Jing, X. B., Biodegradable synthetic polymers: Preparation, functionalization and biomedical application. *Progress in Polymer Science* **2012,** *37* (2), 237-280.

10. (a) Su, M.; Huang, H.; Ma, X.; Wang, Q.; Su, Z., Poly(2-vinylpyridine)-block -Poly(-caprolactone) single crystals in micellar solution. *Macromol. Rapid Commun.* **2013,** *34* (13), 1067-71; (b) Rizis, G.; van de Ven, T. G.; Eisenberg, A., "Raft" formation by two-dimensional self-assembly of block copolymer rod micelles in aqueous solution. *Angew. Chem. Int. Ed.* **2014,** *53* (34), 9000-3; (c) He, W. N.; Xu, J. T.; Du, B. Y.; Fan, Z. Q.; Wang, X. S., Inorganic-Salt-Induced Morphological Transformation of Semicrystalline Micelles of PCL-b-PEO Block Copolymer in Aqueous Solution. *Macromol Chem Phys* **2010,** *211* (17), 1909-1916; (d) Glavas, L.; Olsen, P.; Odelius, K.; Albertsson, A. C., Achieving micelle control through core crystallinity. *Biomacromolecules* **2013,** *14* (11), 4150-6; (e) Du, Z. X.; Xu, J. T.; Fan, Z. Q., Regulation of micellar morphology of PCL-b-PEO block copolymers by crystallization temperature. *Macromol. Rapid Commun.* **2008,** *29* (6), 467-471; (f) Du, Z.-X.; Xu, J.-T.; Fan, Z.-Q., Micellar Morphologies of Poly(ε-caprolactone)-b-poly(ethylene oxide) Block Copolymers in Water with a Crystalline Core. *Macromolecules* **2007,** *40* (21), 7633-7637; (g) Arno, M. C.; Inam, M.; Coe, Z.; Cambridge, G.; Macdougall, L. J.; Keogh, R.; Dove, A. P.; O'Reilly, R. K., Precision Epitaxy for Aqueous 1D and 2D Poly(epsilon-caprolactone) Assemblies. *J. Am. Chem. Soc.* **2017,** *139* (46), 16980-16985; (h) Wang, J.; Lu, Y.; Chen, Y., Fabrication of 2D surface-functional polymer platelets via crystallization-driven self-assembly of poly (ε-caprolactone)-contained block copolymers. *Polymer* **2019,** *160*, 196-203.

11. Ren, L. X.; Hardy, C. G.; Tang, S. F.; Doxie, D. B.; Hamidi, N.; Tang, C. B., Preparation of Side-Chain 18-e Cobaltocenium-Containing Acrylate Monomers and Polymers. *Macromolecules* **2010,** *43* (22), 9304-9310.

12. Zhang, J.; Yan, Y.; Chance, M. W.; Chen, J.; Hayat, J.; Ma, S.; Tang, C., Charged metallopolymers as universal precursors for versatile cobalt materials. *Angew. Chem. Int. Ed.* **2013,** *52* (50), 13387-91.

13. (a) Bittiger, H.; Marchessault, R. H.; Niegisch, W. D., Crystal structure of poly-ε-caprolactone. *Acta Crystallogr. B* **1970,** *26* (12), 1923-1927; (b) Ganda, S.; Dulle, M.; Drechsler, M.; Forster, B.; Forster, S.; Stenzel, M. H., Two-Dimensional Self-Assembled Structures of Highly Ordered Bioactive Crystalline-Based Block Copolymers. *Macromolecules* **2017,** *50* (21), 8544-8553; (c) Jiang, N.; Jiang, S. D.; Hou, Y.; Yan, S. K.; Zhang, G. Z.; Gan, Z. H., Influence of chemical structure on enzymatic degradation of single crystals of PCL-b-PEO amphiphilic block copolymer. *Polymer* **2010,** *51* (11), 2426-2434.

14. Guerin, G.; Rupar, P. A.; Manners, I.; Winnik, M. A., Explosive dissolution and trapping of block copolymer seed crystallites. *Nat. Comm.* **2018,** *9* (1), 1158.

15. Tanaka, H.; Nishi, T., Study of crystallization process of polymer from melt by a real - time pulsed NMR measurement. *J. Chem. Phys.* **1986,** *85* (10), 6197-6209.

16. Zhu, W.; Peng, B.; Wang, J.; Zhang, K.; Liu, L.; Chen, Y., Bamboo leaf-like micro-nano sheets self-assembled by block copolymers as wafers for cells. *Macromol. Biosci.* **2014,** *14* (12), 1764-70.
17. Gratton, S. E.; Ropp, P. A.; Pohlhaus, P. D.; Luft, J. C.; Madden, V. J.; Napier, M. E.; DeSimone, J. M., The effect of particle design on cellular internalization pathways. *Proc. Natl. Acad. Sci. U. S. A.* **2008,** *105* (33), 11613-8.
18. Nazemi, A.; Boott, C. E.; Lunn, D. J.; Gwyther, J.; Hayward, D. W.; Richardson, R. M.; Winnik, M. A.; Manners, I., Monodisperse Cylindrical Micelles and Block Comicelles of Controlled Length in Aqueous Media. *J. Am. Chem. Soc.* **2016,** *138* (13), 4484-93.
19. Yao, K.; Chen, Y.; Zhang, J.; Bunyard, C.; Tang, C., Cationic salt-responsive bottle-brush polymers. *Macromol Rapid Commun* **2013,** *34* (8), 645-51.
20. Cao, L.; Manners, I.; Winnik, M. A., Influence of the Interplay of Crystallization and Chain Stretching on Micellar Morphologies: Solution Self-Assembly of Coil−Crystalline Poly(isoprene-block-ferrocenylsilane). *Macromolecules* **2002,** *35* (22), 8258-8260.
21. Inam, M.; Cambridge, G.; Pitto-Barry, A.; Laker, Z. P. L.; Wilson, N. R.; Mathers, R. T.; Dove, A. P.; O'Reilly, R. K., 1D vs. 2D shape selectivity in the crystallization-driven self-assembly of polylactide block copolymers. *Chem. Sci.* **2017,** *8* (6), 4223-4230.
22. (a) Engler, A. C.; Wiradharma, N.; Ong, Z. Y.; Coady, D. J.; Hedrick, J. L.; Yang, Y.-Y., Emerging trends in macromolecular antimicrobials to fight multi-drug-resistant infections. *Nano Today* **2012,** *7* (3), 201-222; (b) Zou, X.; Zhang, L.; Wang, Z.; Luo, Y., Mechanisms of the Antimicrobial Activities of Graphene Materials. *J. Am. Chem. S.* **2016,** *138* (7), 2064-2077.

TOC Graphic